Variations in H_2 thresholds and growth yields among hydrogenotrophic methanogens relate to different energy conservation strategies

Timothé Philippon [(1)], Jo Philips [(1,2)*]

[(1)] Department of Biological and Chemical Engineering, University of Aarhus, Gustav Wieds Vej 10, 8000 Aarhus C, Denmark

[(2)] Novo Nordisk Foundation CO_2 Research Center (CORC), Gustav Wieds Vej 10, 8000 Aarhus C, Denmark

[*] Corresponding author: jo.philips@bce.au.dk

Abstract

Hydrogenotrophic methanogens are of high environmental and biotechnological relevance, as they convert CO_2 with H_2 into CH_4. Despite their common metabolism, variations among these methanogens likely exist. This study therefore determined the H_2 thresholds and growth yields of nine different hydrogenotrophic methanogens. The H_2 threshold, i.e. the H_2 partial pressure at which H_2 consumption halts, ranged over two orders of magnitude from 1.0 ± 0.5 Pa for *Methanobrevibacter arboriphilus* to 120 ± 10 Pa for *Methanosarcina mazei*. Growth yields ranged from 0.51 ± 0.28 $g_{DCW}\cdot(\text{mol } CH_4)^{-1}$ for *Methanococcus maripaludis* to 5.28 ± 1.25 $g_{DCW}\cdot(\text{mol } CH_4)^{-1}$. In addition, ATP gains, estimated from both the H_2 threshold and growth yield, correlated reasonably well, suggesting that these variations are due to differences in energy conservation strategies. Our results fitted with the classification previously proposed by Thauer[1], dividing hydrogenotrophic methanogens into two distinct groups: methanogens using cytochromes for energy conservation had a high H_2 threshold (> 20 Pa) and high growth yield (> 4.0 $g_{DCW}\cdot(\text{mol } CH_4)^{-1}$), whereas all methanogens without cytochromes had a low H_2 threshold (< 8 Pa) and low growth yield (< 1.7 $g_{DCW}\cdot(\text{mol } CH_4)^{-1}$). Moreover, our H_2 thresholds showed significant additional variations within both groups. Overall, this study found strong variations between hydrogenotrophic methanogens, which are important to understand their environmental prevalence and biotechnological applicability.

Introduction

Hydrogenotrophic methanogenesis is a metabolic pathway used by specific archaeal microbes to produce methane (CH_4) from carbon dioxide (CO_2) and dihydrogen (H_2) for the purpose of energy conservation through the following reaction:

$$CO_2 + 4\ H_2 + n\ ADP + n\ Pi \rightarrow CH_4 + 2\ H_2O + n\ ATP \qquad (1)$$

This metabolism is widely spread in the environment and plays an important role in the global carbon cycle, as methanogens are estimated to convert yearly about one gigaton of carbon into methane [1]. This production of methane is a major issue in the context of climate change, as methane is a potent greenhouse gas. Methanogenesis can also negatively impact steel infrastructure, as certain hydrogenotrophic methanogens induce strong corrosion [2]. Nevertheless, hydrogenotrophic methanogenesis is of huge interest for the development of energy conversion (e.g. power-to-gas) biotechnologies, as methane is a valuable fuel. For instance, bio-methanation is an already advanced technology, converting CO_2-containing gases into methane with the addition of H_2 gas (Reaction 1) [3]. Another notable technology based on hydrogenotrophic methanogens is electro-methanogenesis, in which an electrode is used to generate H_2 *in situ* of a bioreactor [4; 5]. Although the latter technology remains in the early stages of development, its potential is considerable [6; 7]. Because of the technological and environmental importance of methanogenesis, a deep understanding of its metabolism and insights into variations between different methanogenic species are crucial.

All hydrogenotrophic methanogens use a common pathway (Figure 1), consisting of a succession of steps reducing CO_2 to CH_4, using electrons obtained from the oxidation of H_2 and carried by electron shuttles, such as the redox cofactor F_{420}. Besides this common pathway, hydrogenotrophic methanogens vary in the involvement of cytochromes [1]. Two identified protein families named *vht* (or *vho*) and *hdrDE* (containing cytochromes) are only present in microbes that perform cytochromes dependent methanogenesis (Figure 1) [8].

Thauer [1] explained that the presence or absence of those cytochromes affects the amount of ATP (ATP gain or *n*) generated in Reaction 1, with a higher ATP gain when those cytochromes are present (Table 1). Different ATP gains in turn affect various metabolic

63 characteristics of methanogens, including their H_2 threshold and growth yield (Table 1).
64 The H_2 threshold quantifies the H_2 concentration at which H_2 oxidation and therefore
65 methanogenesis halts due to thermodynamic constraints. According to Thauer [1], the
66 H_2 threshold is lower for methanogens without cytochromes in comparison to
67 methanogens with cytochromes (Table 1). Accordingly, the growth yield, i.e. the amount
68 of biomass created per amount of H_2 and CO_2 consumed or CH_4 produced, is expected
69 to be higher with than without cytochromes (Table 1). So far, however, it remains unknown
70 whether additional variations in these metabolic characteristics exist, since a coherent
71 comparison of an extensive number of methanogens has not yet been performed.

72 Thauer had based his growth yield values on just few studies, studying each only one to
73 two methanogenic species (e.g. *Methanosarcina barkeri* [9], *Methanobrevibacter*
74 *arboriphilus* [10] or *Methanobacterium bryantii* [11; 12]). It is unclear whether these
75 studies resulted in comparable results, as different growth media and methods were
76 used. Concerning the H_2 threshold, various studies have been conducted on one to few
77 methanogens, while only one study compared four different methanogens, but could not
78 measure H_2 thresholds below 10 ppm [13]. Feldewert has compiled H_2 thresholds for
79 methanogens obtained by various studies [14], but as the H_2 threshold likely depends on
80 the experimental conditions [15], it is unsure if these values are comparable. Moreover,
81 recently strongly different H_2 thresholds were unexpectedly found for acetogens [16]. It
82 seems thus worthwhile revisiting the H_2 thresholds and growth yields of different
83 methanogens.

84 Furthermore, insights into the H_2 thresholds of different methanogens could be crucial to
85 assess their potential for electro-methanogenesis and role in microbial-induced
86 corrosion. In both cases, whether involving a cathode as in electro-methanogenesis or
87 steel as during corrosion, these surfaces act as extracellular electron donors, from which
88 methanogens can withdraw electrons, using H_2 as main intermediate [17]. Not all
89 hydrogenotrophic methanogens, however, are as effective in this extracellular electron
90 uptake [18]. Besides the involvement of extracellular hydrogenases [19], the H_2 partial
91 pressure was proposed to play a role in variations in electroactivity [15]. Microbes
92 maintaining low H_2 partial pressures likely favor H_2 evolution from the cathode or steel
93 surface, thereby increasing extracellular electron uptake rates. As the H_2 threshold

reflects the lowest H_2 partial pressure a strain can sustain, this parameter is thus likely crucial to understand variations in electroactivity among methanogens.

This study therefore aimed to compare H_2 thresholds and growth yields of nine different strains of mesophilic hydrogenotrophic methanogenic species in similar conditions (Table 2). The selected methanogens include species with and without cytochromes, originating from different environments and spanning various methanogenic genera. In addition, two methanogenic strains known for their strong corrosive behavior were included. For all these strains, the H_2 threshold, the growth yield, as well as the assimilated CO_2 fraction, were determined. Moreover, ATP gain estimates based on either the H_2 threshold or the growth yield were calculated and compared. All these different variables are relevant to assess variations in energy conservation strategies among the selected methanogens, as well as to evaluate their potential for extracellular electron uptake.

Material and methods

Methanogenic strains and culture conditions

This study included nine different methanogens (Table 2). Seven methanogenic strains were ordered from the Leibniz Institute DSMZ, including *Methanococcus maripaludis* (DSMZ 2067 designated as type strain in this study), *Methanolacinia petrolearia* (DSMZ 11571), *Methanobacterium palustre* (DSMZ 3108), *Methanobacterium formicicum* (DSMZ 1535), *Methanosarcina mazei* (DSMZ 2053), *Methanosarcina barkeri* (DSMZ 800) and *Methanobrevibacter arboriphilus* (DSMZ 744). Once received, the strains were transferred to their recommended DSMZ medium (exact composition but without Na_2S, sludge fluid or fatty acid mixture) and stored frozen at – 80 °C in a 2 mL tube with 25% glycerol.

In addition, a culture containing *Methanobacterium* strain IM1 [20; 21] was obtained from Florin Musat (Aarhus University). The culture was inoculated in DSMZ medium 141 (without Na_2S) and was stored frozen at – 80 °C, as described for the other strains. Microscope imaging (Leica ICC50 W, Germany) showed that an additional coccus shaped microbe was present in this culture. Nevertheless, when cultivated in a medium with only H_2 as electron donor (no acetate), the IM1 strain (bacille shape [21]) became dominant. Acetate was thus further omitted from the medium. Therefore, we assume that the measured H_2 threshold was for *Methanobacterium* strain IM1.

Methanococcus maripaludis Mic1c10, was provided as living culture by Amelia-Elena Rotaru (Southern University of Denmark). This strain was cultured in DSMZ medium 141 (recommended for *Methanococcus maripaludis*, but without Na_2S) and stored at – 80 °C. Both *Methanococcus maripaludis* Mic1c10 and *Methanobacterium* strain IM1 are known corrosive methanogens, as previously documented [20; 22; 19; 23].

To start experiments, frozen stocks were revived in their respective DSMZ medium and transferred to the same medium once. When the late exponential growth phase was reached, 10 mL of culture was transferred to a sterile glass tube with conical bottom, which had first been hermetically sealed using a rubber stopper and flushed with N_2. These tubes were then centrifuged at 2500 rpm for 15 minutes. The cell pellet was washed two times using limited medium (described below), before being resuspended in

138 the same limited medium. For the H_2 threshold experiment, this cell suspension was
139 diluted with limited medium until an optical density (OD) between 0.10 and 0.15 was
140 reached. It must be noted that this procedure was used both for strains that grow
141 planktonically or as aggregates (notably *M. barkeri* and *M. mazei*), even though similar OD
142 values in this case likely do not correspond to comparable biomass densities.

143 The limited medium was derived from the DSMZ medium 141 and included 0.34 g of KCl,
144 3.45 g of $MgSO_4$ x 7 H_2O, 4 g of $MgCl_2$, 0.25 g of NH_4Cl, 0.14 g of $CaCl_2$, 0.14 g of K_2HPO_4,
145 0.2 mg of $Fe(NH_4)_2(SO_4)_2$, 0.2 g yeast extract powder (Y1625), 10 mL of Wolin mineral
146 solution 10 mL of Wolin vitamins solution for a final volume of one liter. In addition, NaCl
147 was added for a final concentration of 0.4 g per L or 18 g per L, respectively for freshwater
148 methanogens (*M. palustre, M. formicicum*, *M. barkeri*, *M. arboriphilus* and *M. mazei*) and
149 marine methanogens (*strain IM1*, *M. maripaludis* DSMZ 2067 and Mic1c10 strain and *M.*
150 *petrolearia*) (Table 2). After autoclaving this basal medium, filter-sterile stocks solutions
151 were added for a final concentration of 5 g of $NaHCO_3$ and 0.5 $g.L^{-1}$ of L-cysteine.

152 **Measurement of the H_2 threshold**

153 The H_2 threshold was measured for all methanogenic strains. A volume of 80 mL of the
154 cell suspensions obtained after washing was brought into 250 mL serum bottles. For
155 each strain, four replicates were prepared, while three additional bottles were filled with
156 80 mL of limited medium as abiotic controls. The experiment was initiated by flushing the
157 headspace of the bottles with a gas mix composed of 2 % H_2, 78 % N_2 and 20 % CO_2. This
158 mix was prepared using gas flow meters (Alicat®, MCW Series, USA) with two gas tanks,
159 one containing 80% H_2 and 20% CO_2 and the other containing 80% N_2 and 20 % CO_2. Each
160 serum bottle was pressurized for a total pressure of 2 bars (or 1 bar overpressure) of this
161 gas mix. The bottles were incubated upright at 30 °C with horizontal orbital shaking at 100
162 rpm. The total pressure was measured with a digital manometer (OMEGA DPG108, UK)
163 before each sampling event. The headspace of each bottle was frequently sampled with
164 a syringe for H_2 analysis (1.5 mL). The H_2 threshold was considered reached when the H_2
165 partial pressure did not significantly decrease for at least four days with measurement
166 intervals of maximally two days. The value of the H_2 threshold was calculated from the
167 average of two to four measurements performed during those last four days. After the
168 threshold was reached, the headspace was flushed and pressurized again with the gas

169 mix as described above. The headspace was sampled again until the H_2 threshold was
170 reached for a second time. The OD and the methane content in the headspace were
171 measured at the end of the experiment. For all methanogens, the amount of CH_4 at the
172 end of the H_2 threshold experiment was too low to be accurately quantified, even though
173 detectable by GC.

174 Growth yield measurements

175 In addition to the H_2 threshold, the growth yield of all methanogenic strains was
176 determined. For each methanogen, the inoculum was pre-grown and washed as
177 described above. Four replicated bottles (250 mL) with 80 mL of limited medium were
178 inoculated by injecting 0.5 mL of washed culture. These bottles were pressurized at 2
179 bars (overpressurize of 1 bar) using a gas mix with 80% H_2 and 20 % CO_2. The composition
180 of the headspace was quantified, and the concentration of dissolved inorganic carbon
181 (DIC) in the liquid phase was measured before the start of the incubation. The bottles
182 were incubated upright at 30 °C under horizontal and orbital shaking at 100 rpm. The
183 pressure was measured daily until at least one of the four replicates reached a negative
184 pressure, after which the incubation was ended for all replicates. Before biomass was
185 harvested, the analysis of the headspace composition and determination of the DIC
186 concentration were repeated. Next, the bottles were opened and 10 mL of each culture
187 was transferred into a 20 mL glass tube with conical bottom and centrifuged at 3000 rpm
188 for 15 minutes. The clear supernatant was discarded and an additional 10 mL of culture
189 was placed in the same tube, while keeping the cell pellet. This centrifugation procedure
190 was repeated until all 80 mL of each bottle was harvested. Each of the tubes containing
191 the stacked cell pellets were then dried at 100 °C for 48 hours, cooled down for one hour
192 in a desiccator and the dry weight was measured using an analytical balance (± 0.0001 g
193 precision) (VWR, LD17 4XN). The growth yield was calculated by dividing the dried cell
194 weight by the quantity of methane measured in the headspace at the end of the
195 experiment.

196 Analytical methods

197 Gaseous samples were analyzed for H_2, CH_4 and CO_2 using a Compact GC 4.0
198 (Interscience, Netherlands) with two different columns: one Molsieve 5A 30 m x 0.32 mm

and one Rt-QBond 3 m x 0.32 mm, using helium as gas carrier and a TCD detector [16]. Calibration was performed using calibrating gases mixed with N_2. The quantification limit was 1 Pa or 10 ppm for H_2, 10 000 ppm for CH_4 and 50 ppm for CO_2.

For H_2 partial pressures below 50 ppm, a Peak Performer 1 (PP1) (Peak Laboratories, USA) GC unit based on HgO–Hg conversion with a reducing compound photometer (RCP) was also used. This GC measures trace H_2 levels (0.1–50 ppm of H_2) and has quantification limit well below that of the CompactGC. Partial pressures were calculated by multiplying the mol fraction, as measured by GC, with the total pressure. Dissolved concentrations were calculated from the partial pressures using the Henry constants for H_2 at 30°C (7.8 x 10^{-4} mol.l^{-1}.bar^{-1}) [24].

Liquid samples were prepared for DIC analysis, as previously described [25]. A sample of 0.5 mL was mixed with 0.85 mL of 800 mM HCl in 20 mL closed Hungate tubes, previously flushed with N_2 and kept at atmospheric pressure. The acidified sample was then vortexed for 2 minutes and left to equilibrate for eight hours to convert bicarbonate into CO_2. The CO_2 level in the headspace of the tube was then measured as described above. A calibration curve was prepared prior to the experiment using sodium bicarbonate. Optical densities (OD) were measured at 600 nm using a Denovix DS-11+ spectrophotometer.

Calculations

Estimation of the ATP gain from the H_2 threshold

As explained previously [16], H_2 thresholds can be used to calculate an estimate for the ATP gain through calculating the critical Gibbs free energy, i.e. the Gibbs free energy change when the H_2 threshold is reached [1].

Considering hydrogenotrophic methanogenesis:

$$CO_2 + 4\,H_2 \rightarrow CH_4 + 2\,H_2O \qquad (2)$$

The critical Gibbs free energy (ΔG_c) becomes:

$$\Delta G_c = \Delta G^{0'}_{\text{methanogenesis}} + R \cdot T \cdot \ln \frac{p_{\text{CH}_4}}{p_{\text{CO}_2} * \theta_{\text{H}_2}{}^4} \qquad (3)$$

With $\Delta G^{0'}_{\text{methanogenesis}}$ the Gibbs free energy of methanogenesis (Reaction 2) in physiological standard conditions (-131 kJ.mol^{-1} [1]), θ_{H_2} the H_2 threshold (in atm), p_{CO_2} the partial pressure of CO_2 (in atm) and p_{CH_4} the partial pressure of methane (in atm) at the H_2 threshold. As the methane partial pressures in the H_2 threshold experiment were too low to be quantified, they were calculated from the amount of H_2 consumed, according to the stoichiometric ratios of Reaction 2.

The critical Gibbs free energy at the H_2 threshold is not zero, because methanogenesis should be considered as coupled to ADP to ATP phosphorylation (Reaction 1). At the H_2 threshold, it can be assumed that the total Gibbs free energy change of Reaction 1 considering both methanogenesis and ADP phosphorylation, equals zero [1]:

$$\Delta G_c + n \,.\, \Delta G_{ATP} = 0 \qquad (4)$$

Where ΔG_{ATP} is the Gibbs free energy change for the phosphorylation of ADP into ATP. The value of this ΔG_{ATP} can vary between microorganisms and different values are used in literature [1; 16], but here we used the value of -75 kJ.mol^{-1} [26]. The ATP gain *n, i.e.* the number of ADP molecules phosphorylated for each completed methanogenesis reaction, can finally be calculated using:

$$n = -\frac{\Delta G_c}{\Delta G_{ATP}} \qquad (5)$$

Estimation the ATP gain from the growth yield

In parallel to the calculations from the H_2 thresholds, the ATP gain was also estimated from the experimentally measured growth yields. Spormann [27] described a relationship between the growth yield expressed per catabolic product (in our case methane) (Y^{CH_4}, g dry cell weight per mole of methane) and the growth yield expressed per ATP (Y^{ATP}, g dry cell weight per mole ATP). This relationship can be used to estimate the ATP gain *n* (mole ATP per mole methane):

$$n = \frac{Y^{CH_4}}{Y^{\text{ATP}}} \qquad (6)$$

Y^{ATP} was estimated to be 5 g dry cell weight per mole of ATP for an anabolic metabolism using CO_2 as carbon source [27].

Estimation of the fraction of assimilated carbon

The growth yield experiment also allowed to compare the fraction of CO_2 assimilated into biomass among the different methanogens. The total amount of inorganic carbon consumed by the methanogens was calculated from the headspace CO_2 levels and the DIC concentrations measured at the beginning and the end of the experiment. It was further assumed that methanogenic biomass has the molecular formula of $C_{4.9}H_{9.4}O_{2.9}N$ (molar weight of 129 g per mole), as proposed by Rittmann and McCarty [28]. The amount of moles of assimilated carbon was then calculated from the dry cell weight measured at the end of the experiment.

The fraction of assimilated carbon ($f_{C,biomass}$) was then obtained by dividing the moles of carbon assimilated in biomass ($n_{C,biomass}$) with the total moles of consumed CO_2 ($n_{C,total}$):

$$f_{\mathrm{C,biomass}} = \frac{n_{\mathrm{C,biomass}}}{n_{\mathrm{C,total}}} \cdot 100\% \tag{7}$$

Statistical Analysis

Welch ANOVA test

Welch-Anova tests were performed to differentiate statistically significant groups using both GraphPad Prism® and RStudio (ver. 4.4.3). The Welch test was chosen because the variances were considered too different to perform a regular ANOVA test. All the tests were performed with $\alpha = 0.05$ and the p-value was set at 0.05 for all tests.

Error propagation

Standard deviations on the experimental results were calculated using Excel and were further propagated through the different calculations using available calculators [29; 30].

Results

H_2 threshold measurements

In this study, the H_2 threshold of nine different methanogenic strains was measured, as the H_2 partial pressure at which their H_2 consumption halts. In all abiotic controls, the H_2 partial pressure remained almost stable for the entire duration of the experiment (Figure 2, Figure S1), as only a small drop of the total pressure was observed, as the result of headspace sampling (Figure S1).

For all inoculated bottles, a clear drop in the H_2 partial pressure was observed (Figure 2), confirming H_2 consumption by the different methanogens. Moreover, H_2 consumption halted at a certain H_2 partial pressure for each strain. To confirm these H_2 thresholds, H_2 was reinjected, once stable H_2 partial pressures were reached. For most methanogenic strains, the H_2 thresholds reached after the re-addition of H_2 were comparable to those before the re-addition, except for *Methanosarcina mazei* and *Methanosarcina barkeri* (Figure S2). *M. mazei* consumed H_2 after the H_2 re-addition, but its H_2 consumption halted at a higher H_2 partial pressure (260 ± 49 Pa versus 120 ± 10 Pa before the re-addition). In contrast, *M. barkeri* no longer consumed H_2 after the re-addition. These findings are possibly explained by the exhaustion of these strains over the long incubation time (*M. mazei* reaches its H_2 threshold after 12 days of incubation, while *M. barkeri* required more than 28 days), while all other methanogens, required about five days or less to reach a H_2 partial pressure close to their H_2 threshold.

The three species belonging to the *Methanobacterium* genus displayed similar low H_2 thresholds of around 2 Pa (Figure 2, Figure 3, Table 2). Also, *Methanosarcina petrolearia* and *Methanobrevibacter arboriphilus* reached H_2 thresholds in this range. *M. arboriphilus* was the only species that reached a H_2 partial pressure of 1 Pa (Figure 2, Figure 3, Table 2). The Welch-ANOVA test gathered these five strains with the lowest H_2 thresholds in one statistical group (Figure 3). In contrast, all the other strains had higher H_2 thresholds and were classified as each a significantly different group (Figure 3). The two strains of *Methanococcus maripaludis* displayed H_2 thresholds slightly higher than the five strains with the lowest H_2 thresholds (Figure 2, Figure 3, Table 2). Interestingly, the corrosive strain *Mic1c10* had a significantly lower H_2 threshold (around 4 ± 1 Pa) than the type strain

305 (7 ± 1 Pa). The *Methanosarcina* species differed strongly in their H_2 thresholds, as *M.*
306 *barkeri* had a H_2 threshold of 21 Pa ± 2 Pa, while the highest H_2 threshold was recorded for
307 *M. mazei* (120 ± 10 Pa).

308 No significant growth was observed for any of the inoculated bottles over the course of
309 the experiment, as OD_{600} values remained stable (less than 0.1 increase). For the two
310 *Methanosarcina* strains, which grow both planktonically and as aggregates, the stable
311 OD_{600} cannot be used to claim the absence of growth, but as these strains consumed the
312 least H_2 (highest H_2 thresholds), their growth was likely limited. Methane was detected in
313 the headspace of the inoculated bottles at the end of the experiment, but its levels were
314 too low for an accurate quantification.

315 Growth yield measurements and estimation of the carbon assimilated 316 as biomass

317 In parallel of the H_2 threshold study, all the methanogenic strains were grown in bottles
318 on 80% H_2 and 20% CO_2 to determine their growth yields, as well as their assimilated CO_2
319 percentage. In all these bottles methane levels significantly increased over the
320 incubation period, while H_2 and CO_2 were consumed and cell growth occurred (Table S1).
321 These experimental results were used to calculate the growth yield, i.e. the increase of
322 biomass expressed as gram dry cell weight (g_{DCW}) versus the amount of methane
323 produced. In addition, the assimilated CO_2 fraction, i.e. fraction of CO_2 assimilated in
324 biomass versus total amount of consumed CO_2, was calculated (Figure 4, Table 2).
325 Relatively high variabilities between the replicates were obtained for the growth yields
326 and the assimilated CO_2 percentages (large error bars in Figure 4). This is likely due to the
327 low total weight of dried biomass (in mg) obtained during the growth yield experiment
328 (Table S1), limiting the accuracy of this measurement. In addition, the centrifugation
329 steps were possibly not always as effective in removing cells from the culture
330 suspension, which could also explain the high variability between the replicates.

331 Despite the high variability in the dry cell weight, Welch-ANOVA tests identified two
332 significantly different groups in the growth yields (Figure 4, right). The two
333 *Methanosarcina* strains form one group, with high growth yields of 4.09 ± 1.16 and 5.28 ±
334 1.25 g_{DCW}/mole of CH_4 for *M. barkeri* and *M. mazei* respectively. All other methanogens

had significantly lower growth yields, ranging from 0.51 ± 0.28 g_{DCW}/mole of CH_4 (for *M. maripaludis* type strain) to 1.69 ± 0.58 g_{DCW}/mole of CH_4 (for *M. formicicum*). Growth yields were also expressed as g_{DCW} per mole H_2 or CO_2 consumed (Figure S3), leading two the same statistical groups. Moreover, the same two significantly different groups were also identified for the fraction of assimilated CO_2 percentages (Figure 4, right) with *M. mazei* and *M. barkeri* having a high assimilation percentage, i.e. 22.7 ± 10.0 % for *M. mazei* and t18.9 ± 3.0 % for and *M. barkeri*. All other methanogens displayed a significant lower assimilation percentage, which was 7.15 ± 3.18% for *M. formicicum* and even lower for the other strains.

Comparison ATP gains estimated from either the H_2 threshold or the growth yield

Both the H_2 threshold and the growth yield allow to estimate the ATP gain, i.e. the number of ATP molecules obtained for one complete methanogenesis reaction (Reaction 1). Using the H_2 threshold, the ATP gain estimates ranged from 0.32 ± 0.07 for *M. arboriphilus* to 0.97 ± 0.01 for *M. mazei* (Table 2). Estimating ATP gains from the growth yields gave a slightly wider range, starting at 0.10 ± 0.03 for *M. maripaludis* up to 1.06 ± 0.12 for *M. mazei*. Despite the totally different experimental procedures and calculation methods, both estimates thus led to a largely overlapping range, validating our experimental approach. These ATP gains estimates were further correlated to each other, leading to a clear but not perfect correlation (Figure 5, R^2 of 0.84). Only the two *Methanosarcina* species, *M. mazei* and *M. barkeri,* fall on the 1:1 correlation line, while the correlation is less clear for the other strains. For these other strains, the difference in ATP gain ranges from 0.1 for *M. palustre* to 0.45 for *Methanococcus maripaludis type strain*. Moreover, for these methanogens, higher ATP gains were calculated from the H_2 thresholds than from the growth yield, demonstrating that there were discrepancies between our methods, possibly because the growth yields were somewhat underestimated. This illustrates that our ATP gains should be considered as estimates, rather than absolute values. Nevertheless, the clear correlation (Figure 5) does suggest that the ATP gains differed among the tested strains, reflecting differences in their energy conservation strategies.

Discussion

Variations in the H_2 thresholds and growth yields among methanogens correspond to different energy conservation strategies

This work evaluated the H_2 threshold, growth yield and assimilated CO_2 fraction for nine different methanogenic strains. Experimental H_2 thresholds varied two orders of magnitudes among methanogens, ranging from 1.0 ± 0.5 Pa for *M. arboriphilus* to 120 ± 10 Pa for *M. mazei* (Figure 3, Table 2), which is a similar range as previously recorded [31]. Recorded H_2 thresholds for hydrogenotrophic methanogens are usually not lower than 1 Pa [14], as in our study (Table 2). Only strict methylotrophic methanogens, which use H_2 for the reduction of methyl compounds (in contrast to CO_2 reduction as for hydrogenotrophic methanogens) have H_2 threshold as low as 0.1 Pa [14]. Intriguingly, widely varying H_2 thresholds were previously reported for *M. barkeri* (19 Pa to 150 Pa) [14; 13; 31]. Our experimental H_2 threshold for this strain (21± 2 Pa, Table 2) agrees with the lowest reported value. These variations in reported values are possibly due to different experimental conditions (e.g. different medium composition) [15]. In addition, the slow H_2 consumption by this specific strain (Figure 2) likely makes it hard to conclude when the H_2 threshold is reached. Here, we found that after the halt of H_2 consumption, *M. barkeri* could not be reactivated, while all other methanogens could (Fig S2). Our H_2 threshold for *M. barkeri* could thus still be somewhat overestimated. For *M. mazei*, we measured a six times higher H_2 threshold (120 ± 10 Pa, Table 2) than for *M. barkeri*. *M. mazei* was still active after the H_2 re-addition, so its significantly higher H_2 threshold is not due to an experimental artefact.

Overall, the experimental H_2 thresholds found in this study agree with the classification proposed by Thauer (Table 1), as we found H_2 thresholds below 10 Pa for all methanogens without cytochromes, while methanogens with cytochromes had H_2 thresholds above 10 Pa (Table 2). Nevertheless, in both these groups, we found methanogens with statistically different H_2 thresholds (Figure 3), showing that additional variations in H_2 thresholds exist.

Experimental growth yields varied one order of magnitude among methanogens, ranging from 0.51 ± 0.28 g_{DCW}/mol CH_4 for *M. maripaludis* to 5.28 ± 1.25 g_{DCW}/mol CH_4 for *M.*

395 *mazei*. These growth yields are coherent with what can be found in literature [1; 31]. For
396 instance, Weimer *et al.* reported a growth yield of 6.4 g_{DCW}/mol CH_4 for *M. barkeri*, which
397 is comparable to our growth yield (4.09 ± 1.16 g_{DCW}/mol CH_4, Table 2) [9]. Likewise, our
398 growth yield for *M. arboriphilus* (0.71 ± 0.41 g_{DCW}/mol CH_4) is comparable to the value
399 recorded by Morii et al. (up to 1.42 g_{DCW}/mole of CH_4) [10]. These values do not match
400 perfectly, possibly because growth yields of methanogens depend on the H_2 supply rate
401 [32; 33]. This again highlights the need to compare strains in similar experimental
402 conditions, as in our study.

403 Similar as for the H_2 thresholds, our experimental growth yields agree with the
404 classification proposed by Thauer (Table 1). We indeed found growth yields lower than 3
405 g_{DCW}/mol CH_4 for all methanogens without cytochromes, while the two *Methanosarcina*
406 species (with cytochromes) had growth yields above 3 g_{DCW}/mol CH_4 (Table 2). However,
407 no further significant differences in growth yields were identified in these two groups
408 (Figure 4, left), as was found for the H_2 thresholds (Figure 3). Even for *M. mazei* and *M.*
409 *barkeri*, which differ six times in their H_2 threshold, no significant different growth yields
410 were found (Figure 4). It is likely that this incoherence is due to the high variability of the
411 growth yield measurement (high error bars in Figure 4). Such a high variability is common
412 for growth yield measurements, as it was also observed in previous studies determining
413 methanogenic growth yield [34-37].

414 Thauer [1] did not evaluate possible differences in the fraction of CO_2 assimilated into
415 biomass between methanogens with and without cytochromes. In this study, we did
416 observe two statistically different groups in the assimilated CO_2 fraction, which
417 correlated perfectly with the presence or absence of cytochromes (Figure 4, right).
418 Methanogens without cytochromes assimilated a low fraction of CO_2 (ranging from 1.68
419 ± 0.90% to 7.15 ± 3.18%). In contrast, methanogens with cytochromes assimilated a
420 higher fraction of the converted CO_2 (ranging from 18.97 ± 3.06% to 22.76 ± 10.04%). This
421 difference is not unexpected, as the assimilated CO_2 fraction is closely linked to the
422 growth yield.

423 The experimental H_2 thresholds and growth yields were furtherused to calculate
424 estimates for the ATP gain, to thereby evaluate differences in energy conservation among
425 the tested methanogens. Despite the two totally different experimental approaches and

426 the various assumptions underlying these calculations (Equations 5 and 6), an
427 overlapping range and decent correlation was obtained between the two types of ATP
428 estimates (Table 2, Figure 5), validating our approach.

429 Thauer [1] previously estimated an ATP gain of 1.5 ATP per mol CH_4 for *Methanosarcina*
430 *barkeri* (methanogen with cytochrome), while we calculated this to be 0.75 ± 0.01 ATP per
431 mol CH_4, when derived from the H_2 threshold. However, Thauer used a ΔG_{ATP} of - 50 kJ
432 per mol, while we chose to use a ΔG_{ATP} of - 75 kJ per mole, as this also includes heat loss
433 [26]. According to Thauer (Table 1), methanogens without cytochromes have an ATP gain
434 of 0.5 per mole of CH_4, which corresponds with the range of ATP gain estimates (between
435 0.10 and 0.56 mol ATP per mol CH_4) determined here for methanogens without
436 cytochromes (Table 2).

437 In addition to the clear distinctions between methanogens with and without
438 cytochromes, our ATP gain estimates calculated from the H_2 thresholds suggest that
439 additional variations in energy conservation exist, as additional significant differences in
440 H_2 thresholds were recorded in both the groups of methanogens (Figure 3). Unfortunately,
441 this was not confirmed by the ATP gains derived from the growth yields, again due to the
442 high variability on the growth yield measurements. In conclusion, the presence or
443 absence of cytochromes (use of hdrDE and vhtAGC, versus the use of hdrABC, Figure 1)
444 thus represents two totally different mechanisms for energy conservation in
445 hydrogenotrophic methanogens. Further minor variations likely exist in these energy
446 conservation mechanisms, as reflected by our experimental H_2 thresholds. Further
447 genetic and biochemical analyses will be required to unravel these variations in more
448 detail.

449 Link between the H_2 threshold and extracellular electron uptake by 450 methanogens

451 The H_2 threshold of methanogens is possibly a crucial parameter to understand
452 variations in electroactivity among methanogens, as the rate of extracellular electron
453 uptake from a cathode or steel surface is thought to depend on the H_2 pressure
454 maintained by microbial H_2 consumption [15]. The experimental H_2 thresholds obtained

455 in this study (Table 2, Figure 3) thus allow to reevaluate previously reported differences in
456 electroactivity among methanogens.

457 Mayer et al. studied the electro-methanogenesis performance of several methanogens.
458 *M. maripaludis* and *M. petrolearia*, for which a low H_2 threshold was found here (Figure
459 3), increased cathodic currents (i.e. key signature of extracellular electron uptake), just
460 as several other methanogens without cytochromes. In contrast, *M. mazei*, for which the
461 highest H_2 threshold was recorded (Figure 3), was incapable of electro-methanogenesis
462 [18]. Similarly, Jaramillo *et al*. investigate the corrosion potential of different
463 methanogens [38]. Non-hydrogenotrophic methanogens were reported as non-
464 corrosive, confirming the important role of H_2 as intermediate in microbial corrosion. *M.*
465 *mazei* and *M. barkeri* (high H_2 threshold) were found to be mild corrosive, whereas
466 *Methanobacterium* spp. (low H_2 threshold) were classified as highly corrosive. Overall,
467 these correlations thus suggest that methanogens with a low H_2 threshold have a better
468 ability for extracellular electron uptake than methanogens with a high H_2 threshold.

469 Nevertheless, several other variables likely affect the extracellular electron uptake rate
470 of methanogens, in addition to the H_2 threshold. For instance, the H_2 pressure maintained
471 at the cathode or steel surface also depends on the rate of H_2 consumption. Fast H_2
472 consumption is thus likely also required to maintain low H_2 partial pressures. Moreover,
473 the H_2 evolution reaction on a cathode or steel surface does not only get stimulated by
474 low H_2 levels (thermodynamic effect), but also by extracellular enzymes, such as
475 hydrogenases (kinetic effect). *M. maripaludis* Mic1c10, for instance, has a unique
476 extracellular hydrogenase anchored to its cell surface [22], causing stronger corrosion
477 than other *M. maripaludis* strains [22]. Moreover, the cathodic current increase was
478 double as high for strain Mic1c10 than for a non-corrosive *M. maripaludis* strain [18; 39].
479 Here, we found that strain Mic1c10 had a significantly lower H_2 threshold than the *M.*
480 *maripaludis* wild type (Figure 3, Table 2). Kawachi et al. [22] also recorded that strain
481 Mic1c10 maintained slightly lower H_2 levels during steel corrosion than by the *M.*
482 *maripaludis* type strain. These differences, however, are possibly too small to explain the
483 strong corrosion rates caused by Mic1c10, which is thus likely mostly due to its
484 extracellular hydrogenases. Similarly, *Methanobacterium* -IM1 was more corrosive than
485 other tested methanogens [23], but here we did not find that strain IM1 had a lower H_2

threshold than other tested *Methanobacterium* strains (Figure 2, Table 3). *Methanobacterium* IM1 thus likely also has an additional mechanism to enhance extracellular electron uptake rate, which is likely similar to the one described for *M. maripaludis* Mic1c10.

Overall, we can conclude that the extracellular electron uptake rates of methanogens are inversely proportional to their H_2 threshold (lower H_2 thresholds correspond to higher extracellular electron uptake rates), whereas few methanogens (e.g. *M. maripaludis* Mic1c10, *Methanobacterium* IM1) have a special additional mechanism to increase extracellular electron uptake rates.

Ecological and biotechnological implications of variations among methanogens

This study found important variations in the H_2 thresholds and growth yields among hydrogenotrophic methanogens. We systematically found that methanogens with a low H_2 threshold have a low growth yield, assimilate a low fraction of CO_2 and have a low ATP gain (Table 2). In contrast, methanogens with a high H_2 threshold have a high growth yield, assimilate a larger carbon fraction and have a higher ATP gain (Table 2). This illustrates that hydrogenotrophic methanogens are confronted with a trade-off between the capacity to consume H_2 at trace levels (methanogens without cytochromes), or the ability to grow strongly (high growth yield) with a high energetic efficiency (high ATP gain) (methanogens with cytochromes). This trade-off allows to understand the ecological niche and biotechnological relevance of the different types of methanogens. For instance, Mills *et al.* [40] found that the presence of the *Methanosarcina* genus in electro-methanogenesis systems was correlated to high H_2 levels (reactors with low coulombic efficiency), while the *Methanobacterium* genus was rather correlated to low H_2 levels ((high coulombic efficiency).

In addition, a correlation between the growth yield (high ATP gain) and the growth rate of methanogens would be expected [16]. However, Thauer [1] described that methanogens with cytochromes (high ATP gain) have a lower growth rate (high doubling time) than methanogens without cytochromes (low ATP gain, but low doubling times). Comparing doubling times, however, is possibly not adequate, since methanogens also strongly vary

516 in cell size (large clustered cells for *Methanosarcina* species versus small different
517 shaped cells for other methanogens) [41; 42]. Nevertheless, also in the H_2 threshold
518 experiment of this study, H_2 was faster consumed by methanogens without cytochromes,
519 than by methanogens with cytochromes (Figure 2). This observation possibly reflects that
520 *Methanosarcina* species are not well adapted to consume H_2. Indeed, these
521 methanogens are not strict hydrogenotrophic, but are also capable of acetoclastic
522 methanogenesis, in contrast to the other tested methanogens. Methanogens with
523 cytochromes are thus possibly mainly adapted to use other substrates than H_2 and only
524 shift to H_2 consumption at high H_2 partial pressures. Overall, future studies comparing
525 the growth and H_2 consumption rates of a wide range of different methanogens in
526 comparable conditions would be highly valuable to unravel these differences.

527 This study only included mesophilic methanogens. A similar comparison as in this study
528 could also be relevant for thermophilic methanogens, because of their high
529 biotechnological importance [43]. Their metabolic properties can most likely already be
530 assessed from the presence or absence of cytochromes in their genome. Interestingly,
531 Thauer (ref) stated that methanogens without cytochromes dominate at thermophilic
532 conditions, while methanogens with cytochromes rather occur at lower temperatures.

533 In this study, we found that H_2 thresholds of methanogens range over two orders of
534 magnitude (Figure 3). In comparison, we previously found three orders of magnitude
535 difference in the H_2 thresholds of acetogenic bacteria (6 Pa to 1990 Pa) [16]. It is often
536 assumed that acetogens cannot compete with methanogens for low H_2 levels, as the
537 latter have lower H_2 thresholds [44]. Our results, however, demonstrate that such a
538 competition rather should be evaluated on species level. For instance,
539 *Methanobacterium* strains indeed have lower H_2 thresholds than *Acetobacterium* spp,
540 but acetogenic *Sporomusa* spp. have H_2 thresholds in the range of those of methanogens
541 without cytochromes and well below those with cytochromes. The outcome of
542 competition for trace H_2 levels between methanogens and acetogens likely also depends
543 on the H_2 consumption rates. Recently, H_2 consumption by acetogens was described by
544 first order kinetics (increasing rates at increasing H_2 levels) [45], while the kinetics of H_2
545 consumption by methanogens rather follows Monod kinetics with low half-saturation
546 constants [46] or even zero-order kinetics [47]. Based on these kinetic differences,

547 methanogens (without cytochromes) consume H_2 likely faster at low H_2 levels, while
548 acetogens have a faster H_2 consumption at higher H_2 levels, even though H_2 consumption
549 rates can still widely vary within these groups [45]. Moreover, also the temperature and
550 pH affect the competition for H_2 between acetogens and methanogens [1; 46; 48; 49; 44;
551 50-52]. Detailed insights into the differences in H_2 consumption among methanogens
552 and between methanogens and acetogens are crucial to assess competition for H_2 in the
553 environment, as well as in mixed culture bioreactor systems, as in anaerobic digestion
554 MES and bio-methanation.

555 **Conclusion**

556 This study demonstrated that the H_2 thresholds, growth yields and assimilated CO_2
557 fractions of nine hydrogenotrophic methanogens varied widely. These differences are
558 related to variations in energy conservation and represent a trade-off among
559 hydrogenotrophic methanogens. Methanogens without cytochromes sustain
560 methanogenesis at low H_2 levels but have low growth yields and ATP gains, while
561 methanogens using cytochromes for energy conservation require higher H_2 levels but
562 achieve higher growth yields and ATP gains. In addition to this distinction based on
563 cytochromes, our results suggest additional metabolic variations, warranting further
564 investigations. Overall, the differences identified here are important to explain the
565 ecological distributions of hydrogenotrophic methanogens, as well as their ability to
566 increase microbial induced corrosion and cathodic electron uptake.

567

Acknowledgement

This study was financed by a Villum Young Investigator grant (VIL53083). We would like to thank Satoshi Kawaichi and Amelia-Elena Rotaru from the University of Southern Denmark for providing the living culture of *Methanococcus maripaludis* Mic1cc10 and Florin Musat from Aarhus University for providing the living culture of *Methanobacterium* IM1. We also acknowledge the Section for Microbiology at Aarhus University for lending their Peak Performer. Heidi Skov Johansen and Laura Mũnoz-Duarte are thanked for their practical support during the experiments and calculations. We also appreciate the advice of Sanne Sandberg Overby on the statistical tests.

Figures

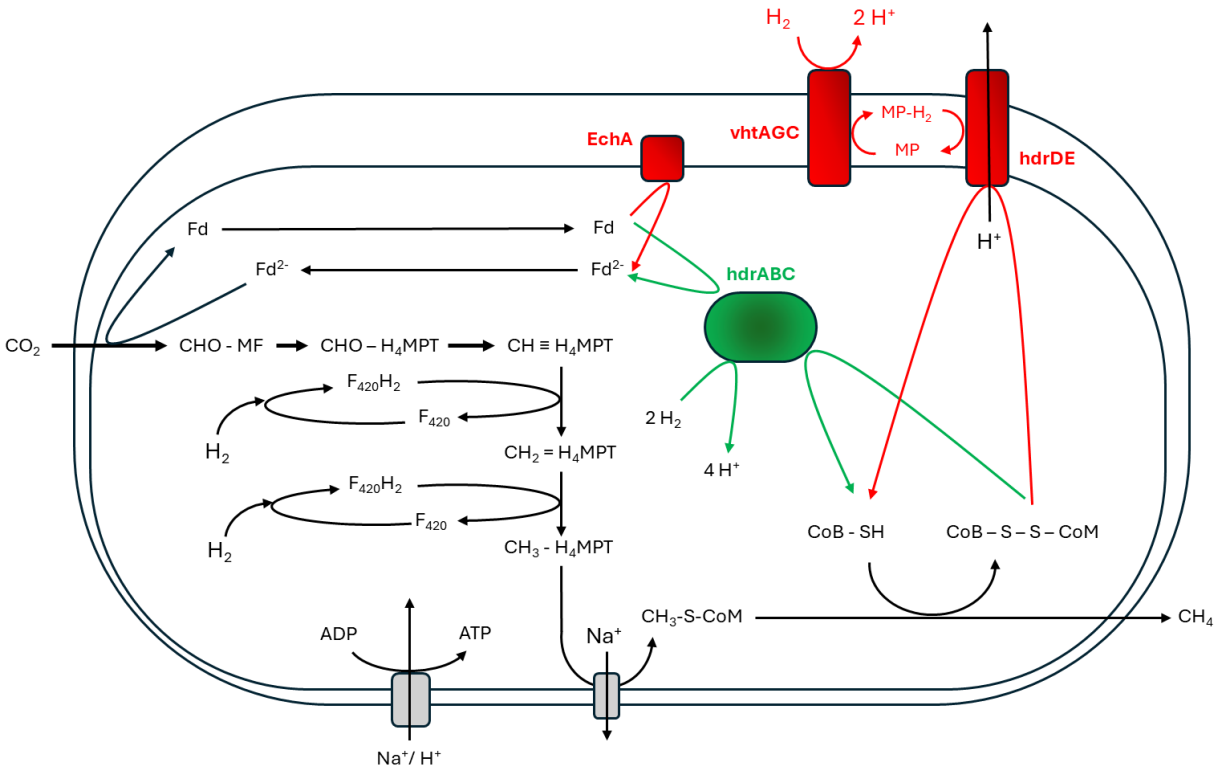

Figure 1: Hydrogenotrophic methanogenesis metabolism. Black colored components and reactions are common for all hydrogenotrophic methanogens. Red colored components are specific for cytochrome-dependent methanogens, which have the two proteins complex *hrdDE* (methanophazine-dependent heterodisulfide reductase) and *vhtAGC* (methanophenazine-reducing hydrogenase). Green colored components only occur in methanogens without cytochromes using the *hdrABC* complex [8; 53; 54].

586 Table 1: Comparison of metabolic characteristics of hydrogenotrophic methanogens depending on the
587 presence or absence of cytochromes according to Thauer [1]:

	Methanogens without cytochromes	Methanogens with cytochromes
H_2 Threshold	Under 10 Pa	Above 10 Pa
Growth yield	Up to 3 g CDW per mol CH_4	Up to 7 g CDW per mol CH_4
ATP gain	0.5 mol ATP per mol CH_4	1.5 mol ATP per mol CH_4
Example of methanogenic orders	*Methanococcus, Methanobrevibacter, Methanobacterium*	*Methanosarcina*

588

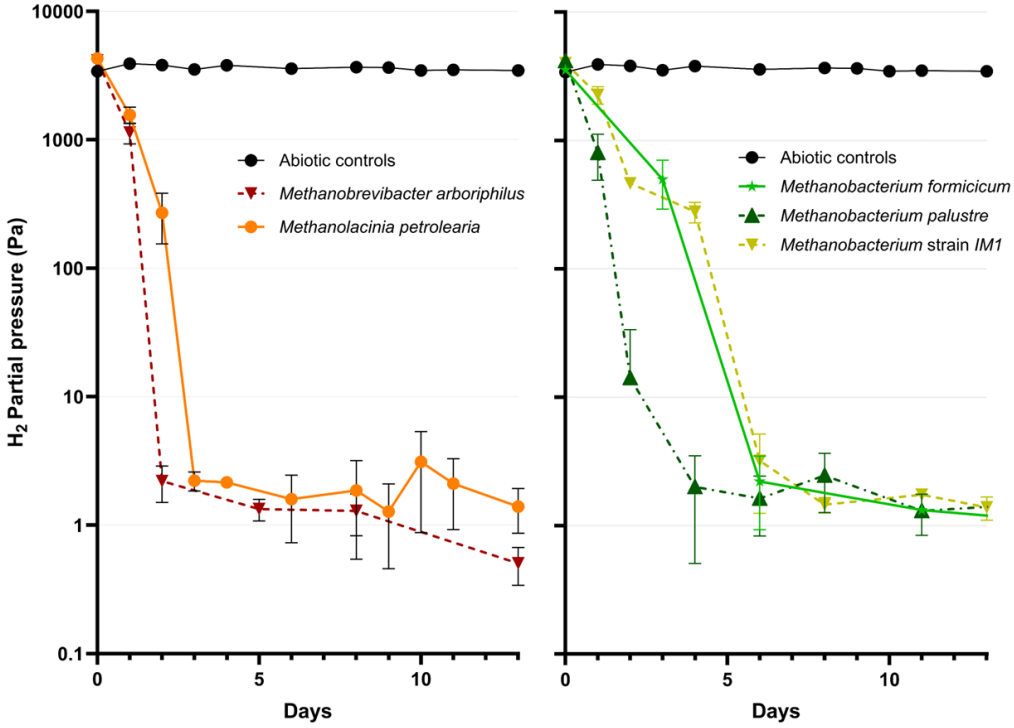

589

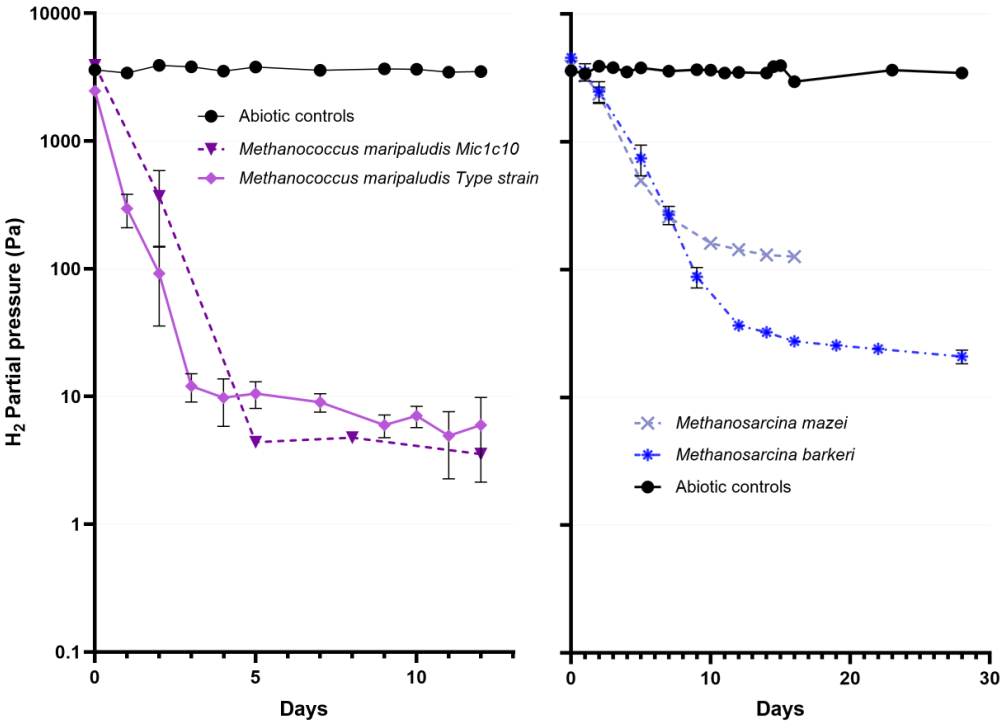

590

591 Figure 2: Change of the H_2 partial pressure (Pa) over time in the H_2 threshold experiment for the nine
592 methanogenic species and compared to the abiotic controls. The data points represent the average of four
593 replicates; the error bars show the standard deviations. Only datapoints before the re-addition of H_2 are
594 shown, later datapoints are shown in Figures S1 and S2.

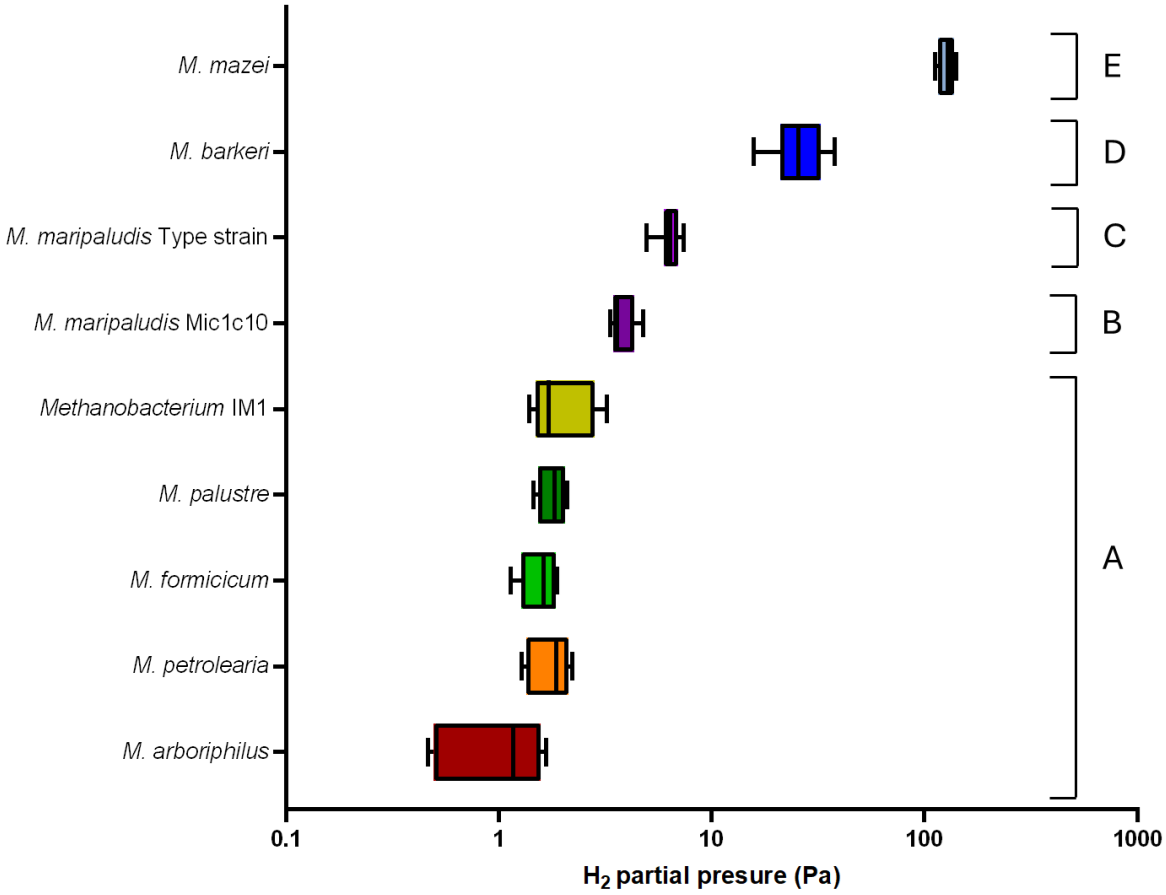

Figure 3: Box plots summarizing the experimental H_2 threshold values for the nine methanogenic strains. The letters indicate statistically different groups, as determined using a Welch-ANOVA test.

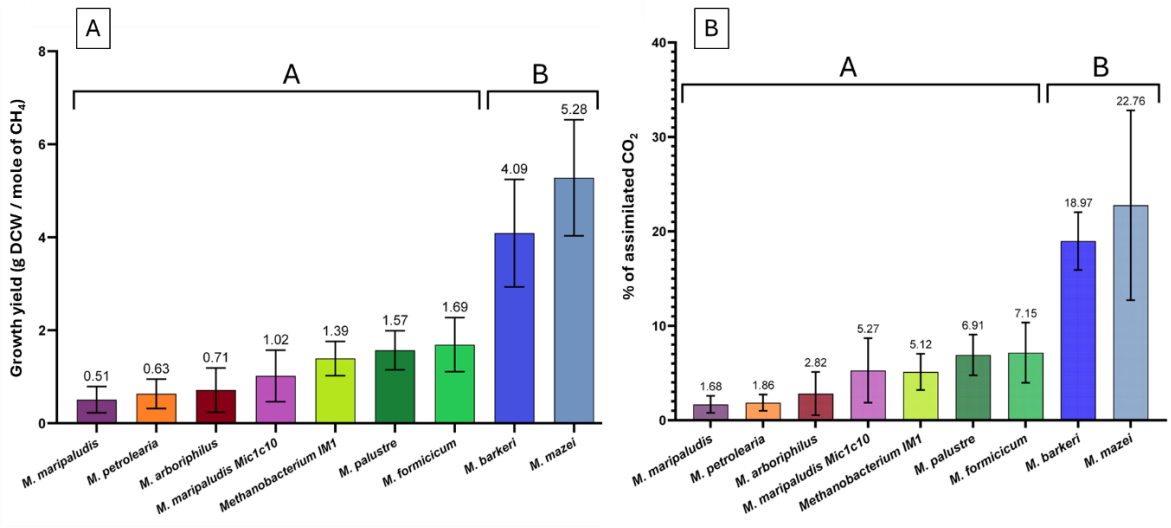

Figure 4: (A) Comparison of the growth yields expressed as the increase of gram Dry Cell Weight (g_{DCW}) per mole of methane produced for the different methanogenic strains (B) Comparison of the estimated percentage of CO_2 assimilated into biomass for the different methanogenic strains. The letters indicate statistically different groups, as determined using a Welch-ANOVA test.

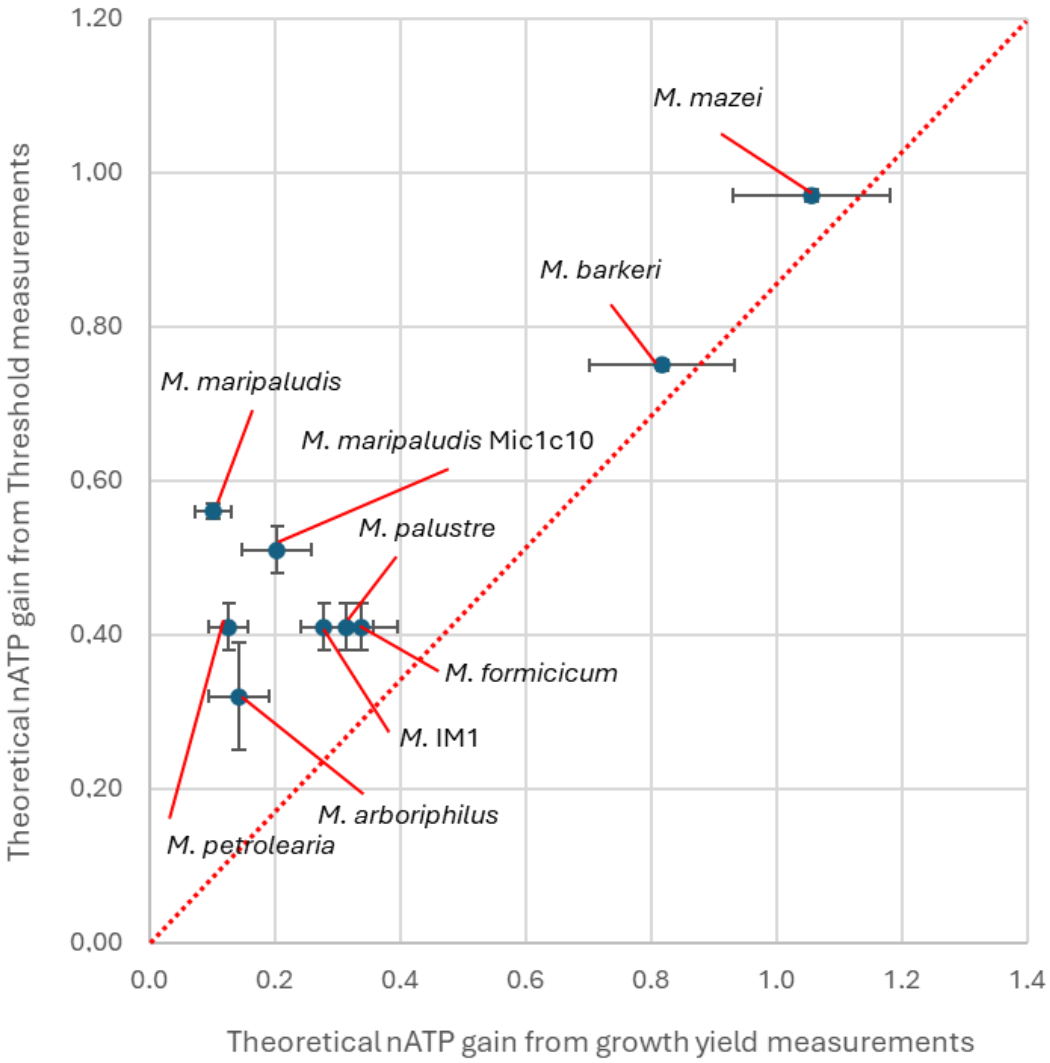

605

606 Figure 5: Correlation of the ATP gains estimations from the experimental H_2 thresholds versus the ATP gains
607 estimated from the experimental growth yields. The vertical and horizontal error bars reflect the standard
608 deviation on these estimates and were propagated from the experimental errors. The red line indicates a
609 1:1 correlation. The correlation coefficient (R2) was 0.84.

610

611 Table 2: Overview of the methanogenic strains examined in this study, as well as their experimentally determined H_2 thresholds, growth yields and assimilated CO_2
612 %. The table also includes the ATP gains estimated either from the experimental H_2 thresholds or the experimental growth yields. The H2 thresholds measured are
613 expressed as partial pressures in the headspace (both in ppm and Pa) and as concentration dissolved in the liquid phase (nM).

Methanogenic strain	Cytochromes	Salinity level	H_2 Threshold			Growth yield	Assimilated CO_2 %	ATP gain estimated from H_2 threshold	ATP gain estimated from growth yield
			ppm	Pa	nM	g_{DCW} (mol CH_4)$^{-1}$		mol ATP (mol CH_4)$^{-1}$	mol ATP (mol CH_4)$^{-1}$
Methanobrevibacter arboriphilus	No [55; 56]	Fresh water	7 ± 1	1.0 ± 0.5	8 ± 3	0.71 ± 0.47	2.82 ± 2.30	0.32 ± 0.07	0.14 ± 0.05
Methanolacinia petrolearia	No [55]	Marine water	10 ± 3	2.0 ± 0.5	16 ± 4	0.63 ± 0.31	1.86 ± 0.86	0.41 ± 0.03	0.13 ± 0.03
Methanobacterium palustre	No [55]	Fresh water	11 ± 2	2.0 ± 0.5	16 ± 4	1.57 ± 0.41	6.91 ± 2.15	0.41 ± 0.03	0.31 ± 0.04
Methanobacterium IM1	No [55]*	Marine water	9 ± 1	2.0 ± 0.5	16 ± 4	1.39 ± 0.36	5.12 ± 1.92	0.41 ± 0.03	0.28 ± 0.04
Methanobacterium formicicum	No [55]	Fresh water	10 ± 1	2.0 ± 0.5	16 ± 4	1.69 ± 0.58	7.15 ± 3.18	0.41 ± 0.03	0.34 ± 0.06
Methanococcus maripaludis Mutant strain Mic1c10	No [55; 53]	Marine water	17 ± 3	4.0 ± 1.0	31 ± 8	1.02 ± 0.55	5.27 ± 3.42	0.51 ± 0.03	0.20 ± 0.05
Methanococcus maripaludis Type strain	No [55; 53]	Marine water	33 ± 4	7.0 ± 1.0	47 ± 12	0.51 ± 0.28	1.68 ± 0.90	0.56 ± 0.01	0.10 ± 0.03
Methanosarcina barkeri	Yes [8; 55]	Fresh water	158 ± 18	21 ± 2	195 ± 31	4.09 ± 1.16	22.76 ± 10.04	0.75 ± 0.01	0.82 ± 0.11
Methanosarcina mazei	Yes [8; 55; 56]	Fresh water	720 ± 20	120 ± 10	936 ± 78	5.28 ± 1.25	18.97 ± 3.06	0.97 ± 0.01	1.06 ± 0.12

614 * The assertion that *Methanobacterium* IM1 does not possess cytochrome is based in the fact that no other *Methanobacterium* was found to have cytochromes.

References

[1] Thauer, Kaster, Seedorf, Buckel, and Hedderich (2008) Methanogenic archaea: ecologically relevant differences in energy conservation. *Nat Rev Microbiol* **6**: 579-591.

[2] An, B.A., Deland, E., Sobol, O., Yao, J.Z., Skovhus, T.L., and Koerdt, A. (2021) The differences in the corrosion product compositions of Methanogen-induced microbiologically influenced corrosion (Mi-MIC) between static and dynamic growth conditions. *Corrosion Science* **180**.

[3] Jensen, M.B., Ottosen, L.D.M., and Kofoed, M.V.W. (2021) H_2 gas-liquid mass transfer: A key element in biological Power-to-Gas methanation. *Renewable & Sustainable Energy Reviews* **147**.

[4] Cheng, S.A., Xing, D.F., Call, D.F., and Logan, B.E. (2009) Direct biological conversion of electrical current into methane by Electromethanogenesis. *Environmental Science & Technology* **43**: 3953-3958.

[5] Palacios, P.A., Philips, J., Bentien, A., and Kofoed, M.V.W. (2024) Relevance of extracellular electron uptake mechanisms for electromethanogenesis applications. *Biotechnology Advances* **73**.

[6] Pandit (2024) Wired for energy: Electromethanogenesis redefining anaerobic digestion. *Process Safety and Environmental Protection*.

[7] Blasco-Gómez, R., Batlle-Vilanova, P., Villano, M., Balaguer, M.D., Colprim, J., and Puig, S. (2017) On the edge of research and technological application: a critical review of Electromethanogenesis. *International Journal of Molecular Sciences* **18**.

[8] Mand, T.D., and Metcalf, W.W. (2019) Energy conservation and hydrogenase function in Methanogenic Archaea, in oarticular the genus *Methanosarcina*. *Microbiol Mol Biol Rev* **83**.

[9] Weimer, P.J., and Zeikus, J.G. (1978) One carbon metabolism in Methanogenic bacteria - cellular characterization and growth of *Methanosarcina barkeri*. *Archives of Microbiology* **119**: 49-57.

[10] Morii, H., Koga, Y., and Nagai, S. (1987) Energetic analysis of the growth of *Methanobrevibacter Arboriphilus* A2 in hydrogen-limited continuous cultures. *Biotechnology and Bioengineering* **29**: 310-315.

[11] Karadagli, F., and Rittmann, B.E. (2005) Kinetic characterization of *Methanobacterium bryantii* M.o.H. *Environmental Science & Technology* **39**: 4900-4905.

[12] Karadagli, F., Marcus, A., and Rittmann, B.E. (2023) Microbiological hydrogen (H_2) thresholds in anaerobic continuous-flow systems: Effects of system characteristics. *Biotechnol Bioeng* **120**: 1844-1856.

[13] Kral, T.A., Brink, K.M., Miller, S.L., and McKay, C.P. (1998) Hydrogen consumption by methanogens on the early Earth. *Orig Life Evol Biosph* **28**: 311-319.

[14] Feldewert, C., Lang, K., and Brune, A. (2020) The hydrogen threshold of obligately methyl-reducing methanogens. *FEMS Microbiol Lett* **367**.

[15] Philips, J. (2019) Extracellular electron uptake by acetogenic bacteria: Does H_2 consumption favor the H_2 evolution reaction on a cathode or metallic iron? *Front Microbiol* **10**: 2997.

[16] Muñoz, L., and Philips, J. (2023) No acetogen is equal: Strongly different H_2 thresholds reflect diverse bioenergetics in acetogenic bacteria. *Environmental Microbiology* **25**: 2032-2040.

[17] Pandit, S., Pandit, C., Mathuriya, A.S., Chatterjee, S., Jadhav, D.A., Yadav, K.K., and Khalid, M. (2024) Wired for energy: Electromethanogenesis redefining anaerobic digestion. *Process Safety and Environmental Protection* **185**: 588-601.

[18] Mayer, F., Enzmann, F., Lopez, A.M., and Hohmann, D. (2019) Performance of different methanogenic species for the microbial electrosynthesis of methane from carbon dioxide. *Bioresource Technology* **289**.

[19] Tsurumaru, H., Ito, N., Mori, K., Wakai, S., Uchiyama, T., Iino, T. et al. (2018) An extracellular [NiFe] hydrogenase mediating iron corrosion is encoded in a genetically unstable genomic island in *Methanococcus maripaludis*. *Sci Rep* **8**: 15149.

[20] Holmes, D.E., Woodard, T.L., Smith, J.A., Musat, F., and Lovley, D.R. (2024) Electrobiocorrosion by microbes without outer-surface cytochromes. *mLife* **3**: 110-118.

[21] Tamisier, M., Schmidt, M., Vogt, C., Kummel, S., Stryhanyuk, H., Musat, N. et al. (2022) Iron corrosion by methanogenic archaea characterized by stable isotope effects and crust mineralogy. *Environ Microbiol* **24**: 583-595.

[22] Kawaichi, S., Kotoky, R., Fiutowski, J., and Rotaru, A.E. (2024) Adaptation of a methanogen to Fe(0) corrosion via direct contact. *NPJ Biofilms Microbiomes* **10**: 100.

[23] Dinh, H.T., Kuever, J., Mussmann, M., Hassel, A.W., Stratmann, M., and Widdel, F. (2004) Iron corrosion by novel anaerobic microorganisms. *Nature* **427**: 829-832.

[24] Sander, R. (2015) Compilation of Henry's law constants (version 4.0) for water as solvent *Atmospheric Chemistry and Physics* **Volume 15**.

[25] Callander, G., Deutzmann, J.S., and Spormann, A.M. (2024) Alkaline hydrogenotrophic methanogenesis in *Methanococcus vannielii* at low carbon dioxide concentrations. *Journal of Co2 Utilization* **83**.

[26] Schink, B. (1997) Energetics of syntrophic cooperation in methanogenic degradation. *Microbiol Mol Biol Rev* **61**: 262-280.

[27] Spormann, A.M., and SpringerLink (2023) nATP and Growth Yields Y_s and Y_{ATP}. In *Principles of Microbial Metabolism and Metabolic Ecology*. Cham: Springer International Publishing : Imprint: Springer, pp. 48-50.

[28] Rittmann, B.E., McCarty, P.L., and AccessEngineering (2020) An empirical formula for microbial cells. In *Environmental biotechnology : principles and applications*. New York, N.Y: McGraw-Hill Education, pp. 144-148.

[29] Lopes, J. URL https://errorpropagation.com/

[30] Truong, Q. URL https://uncertaintycalculator.com/

[31] Kaster, A.K., Moll, J., Parey, K., and Thauer, R.K. (2011) Coupling of ferredoxin and heterodisulfide reduction via electron bifurcation in hydrogenotrophic methanogenic archaea. *Proc Natl Acad Sci U S A* **108**: 2981-2986.

[32] Costa, K.C., Yoon, S.H., Pan, M., Burn, J.A., Baliga, N.S., and Leigh, J.A. (2013) Effects of H_2 and formate on growth yield and regulation of methanogenesis in *Methanococcus maripaludis*. *J Bacteriol* **195**: 1456-1462.

[33] de Poorter, L.M., Geerts, W.J., and Keltjens, J.T. (2007) Coupling of *Methanothermobacter thermautotrophicus* methane formation and growth in fed-batch and continuous cultures under different H_2 gassing regimens. *Appl Environ Microbiol* **73**: 740-749.

[34] Mladenovska, Z., and Ahring, B.K. (2000) Growth kinetics of thermophilic

spp. isolated from full-scale biogas plants treating animal manures. *Fems Microbiology Ecology* **31**: 225-229.

[35] Richards, M.A., Lie, T.J., Zhang, J., Ragsdale, S.W., Leigh, J.A., and Price, N.D. (2016) Exploring hydrogenotrophic methanogenesis: a genome scale metabolic reconstruction of *Methanococcus maripaludis*. *J Bacteriol* **198**: 3379-3390.

[36] Laguillaumie, L., Peyre-Lavigne, M., Grimalt-Alemany, A., Gavala, H.N., Skiadas, I.V., Paul, E., and Dumas, C. (2023) Controlling the microbial competition between hydrogenotrophic methanogens and homoacetogens using mass transfer and thermodynamic constraints. *Journal of Cleaner Production* **414**.

[37] Leggieri, P.A., Kerdman-Andrade, C., Lankiewicz, T.S., Valentine, M.T., and O'Malley, M.A. (2021) Non-destructive quantification of anaerobic gut fungi and methanogens in co-culture reveals increased fungal growth rate and changes in metabolic flux relative to mono-culture. *Microb Cell Fact* **20**: 199.

[38] Jaramillo, P.A.P. (2019) Microbial induced corrosion by methanogens and other associated microbial groups. In *Nordcee, department of Biology*: University of Southern Denmark, pp. 90 - 108.

[39] Mayer, F., Sabel-Becker, B., and Holtmann, D. (2022) Enhanced electron uptake and methane production by corrosive methanogens during Electromethanogenesis. *Microorganisms* **10**.

[40] Mills, S., Dessi, P., Pant, D., Farras, P., Sloan, W.T., Collins, G., and Ijaz, U.Z. (2022) A meta-analysis of acetogenic and methanogenic microbiomes in microbial electrosynthesis. *NPJ Biofilms Microbiomes* **8**: 73.

[41] Boone, D.R. Methanobacterium. In *Bergey's Manual of Systematics of Archaea and Bacteria*, pp. 1-8.

[42] Sowers, K.R., Boone, J.E., and Gunsalus, R.P. (1993) Disaggregation of *Methanosarcina spp*. and growth as single cells at elevated osmolarity. *Appl Environ Microbiol* **59**: 3832-3839.

[43] Angelidaki, I., Karakashev, D., Batstone, D.J., Plugge, C.M., and Stams, A.J. (2011) Biomethanation and its potential. *Methods Enzymol* **494**: 327-351.

[44] Tsapekos, P., Alvarado-Morales, M., and Angelidaki, I. (2022) H_2 competition between homoacetogenic bacteria and methanogenic archaea during biomethanation from a combined experimental-modelling approach. *Journal of Environmental Chemical Engineering* **10**.

[45] Munoz-Duarte, L., Chakraborty, S., Gron, L.V., Bambace, M.F., Catalano, J., and Philips, J. (2025) H_2 consumption by various acetogenic bacteria follows First-Order Kinetics up to H_2 Saturation. *Biotechnol Bioeng* **122**: 804-816.

[46] Kotsyurbenko, O.R., Glagolev, M.V., Nozhevnikova, A.N., and Conrad, R. (2001) Competition between homoacetogenic bacteria and methanogenic archaea for hydrogen at low temperature. *FEMS Microbiology Ecology* **38**: 153-159.

[47] Ripoll, E., Lopez, I., and Borzacconi, L. (2020) Hydrogenotrophic activity: A tool to evaluate the kinetics of methanogens. *J Environ Manage* **270**: 110937.

[48] Conrad, R., and Wetter, B. (1990) Influence of temperature on energetics of hydrogen metabolism in homoacetogenic, methanogenic, and other anaerobic-bacteria. *Archives of Microbiology* **155**: 94-98.

[49] Fu, B., Jin, X., Conrad, R., Liu, H., and Liu, H. (2019) Competition between chemolithotrophic acetogenesis and hydrogenotrophic Methanogenesis for exogenous

750 H_2/CO_2 in anaerobically digested sludge: impact of temperature. *Front Microbiol* **10**:
751 2418.

752 [50] Molenaar, S.D., Saha, P., Mol, A.R., Sleutels, T.H.J.A., ter Heijne, A., and Buisman,
753 C.J.N. (2017) Competition between methanogens and acetogens in biocathodes: A
754 comparison between potentiostatic and galvanostatic control. *International Journal of*
755 *Molecular Sciences* **18**.

756 [51] Le Van, T.D., Robinson, J.A., Ralph, J., Greening, R.C., Smolenski, W.J., Leedle, J.A.,
757 and Schaefer, D.M. (1998) Assessment of reductive acetogenesis with indigenous
758 ruminal bacterium populations and *Acetitomaculum ruminis*. *Appl Environ Microbiol* **64**:
759 3429-3436.

760 [52] Leclerc, M., Bernalier, A., Donadille, G., and Lelait, M. (1997) H_2/CO_2 metabolism in
761 acetogenic bacteria isolated from the human colon. *Anaerobe* **3**: 307-315.

762 [53] Goyal, N., Zhou, Z., and Karimi, I.A. (2016) Metabolic processes of *Methanococcus*
763 *maripaludis* and potential applications. *Microb Cell Fact* **15**: 107.

764 [54] Spormann, A.M., and SpringerLink (2023) *Principles of Microbial Metabolism and*
765 *Metabolic Ecology*. Cham: Springer International Publishing : Imprint: Springer.

766 [55] Ou, Y.F., Dong, H.P., McIlroy, S.J., Crowe, S.A., Hallam, S.J., Han, P. et al. (2022)
767 Expanding the phylogenetic distribution of cytochrome b-containing methanogenic
768 archaea sheds light on the evolution of methanogenesis. *ISME J* **16**: 2373-2387.

769 [56] Kuhn, W., Fiebig, K., Hippe, H., Mah, R.A., Huser, B.A., and Gottschalk, G. (1983)
770 Distribution of cytochromes in methanogenic bacteria. *Fems Microbiology Letters* **20**:
771 407-410.

772

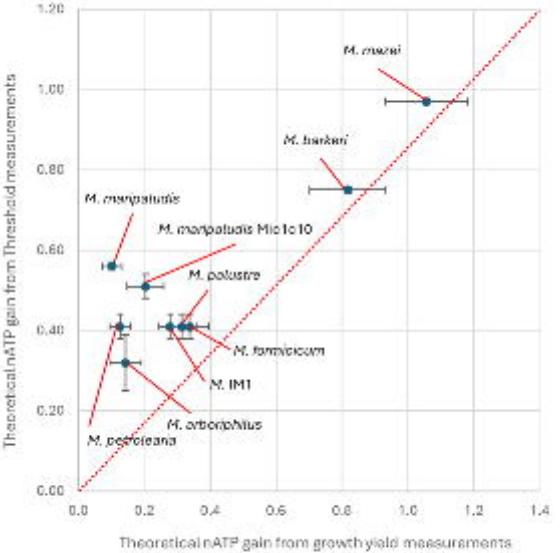
M. mazei
M. barkeri
M. marpaludis
M. marpaludis Mic1c10
M. palustre
M. formicicum
M. IM1
M. arbophilus
M. petroleana
1.20
1.00
0.80
0.60
0.40
0.20
0.00
0.0
0.2
0.4
0.6
0.8
1.0
1.2
1.4
Theoretical nATP gain from Threshold measurements
Theoretical nATP gain from growth yield measurements

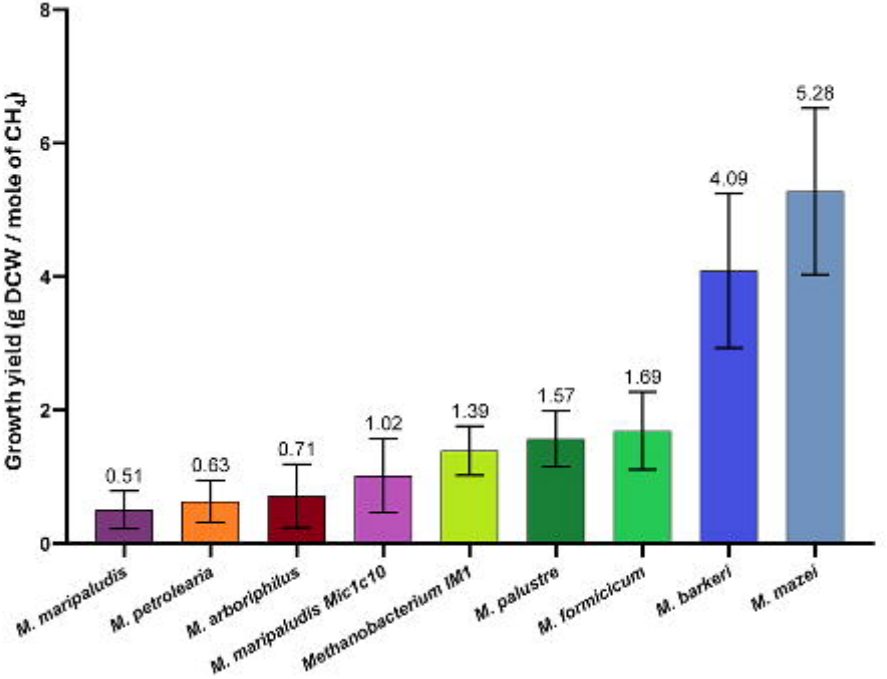
Growth yield (g DCW / mole of CH_4)
0
2
4
6
8
0.51
0.63
0.71
1.02
1.39
1.57
1.69
4.09
5.28
M. maripaludis
M. petroleania
M. arboriphilus
M. maripaludis Mic1c10
Methanobacterium IM1
M. palustre
M. formicicum
M. barkeri
M. mazei

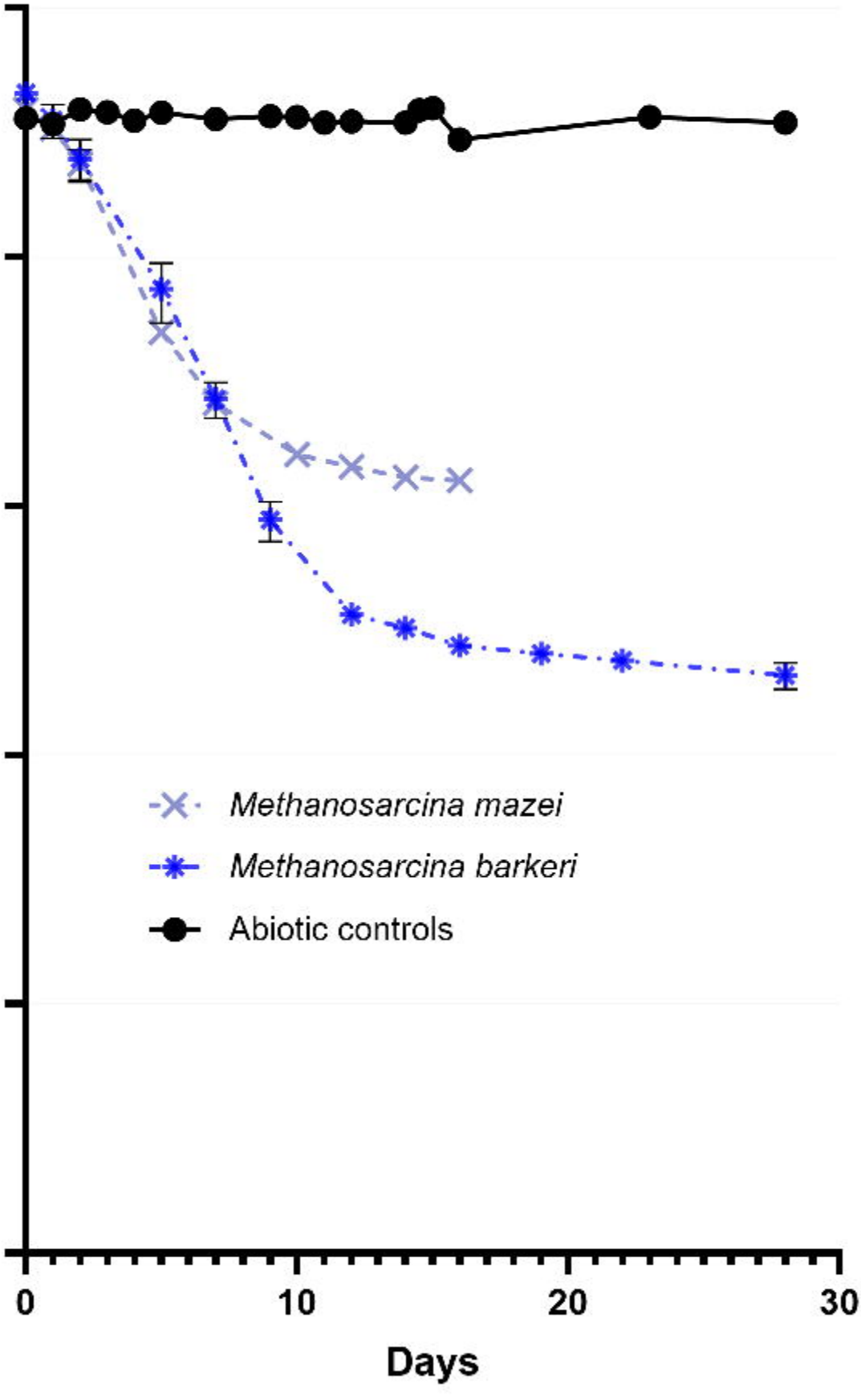
Methanosarcina mazei
Methanosarcina barkeri
Abiotic controls
0
10
20
30
Days

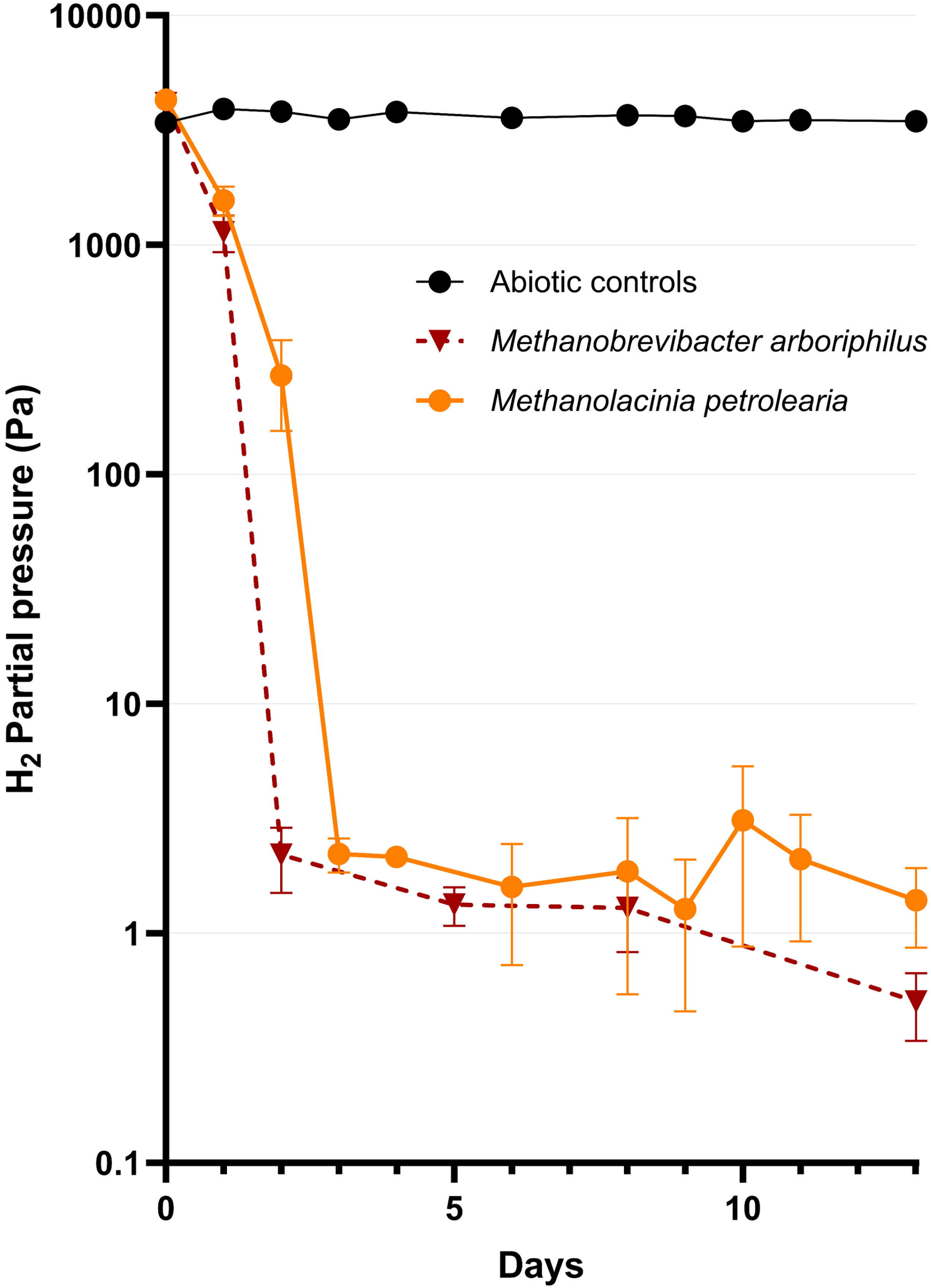
10000
1000
100
10
1
0.1
H_2 Partial pressure (Pa)
0
5
10
Days
Abiotic controls
Methanobrevibacter arboriphilus
Methanolacinia petrolearia

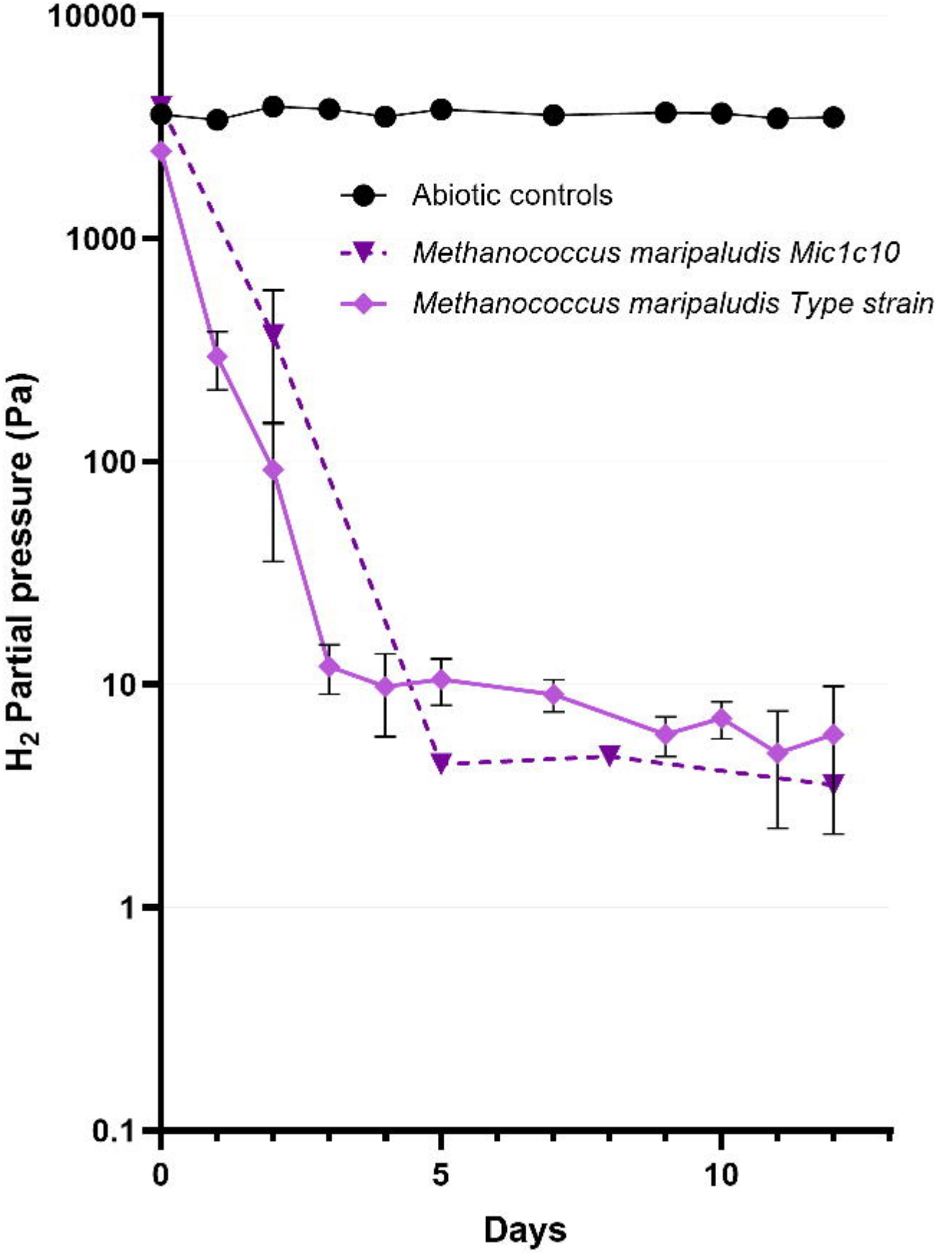
10000
1000
100
10
1
0.1
H_2 Partial pressure (Pa)
0
5
10
Days
Abiotic controls
Methanococcus maripaludis Mic1c10
Methanococcus maripaludis Type strain

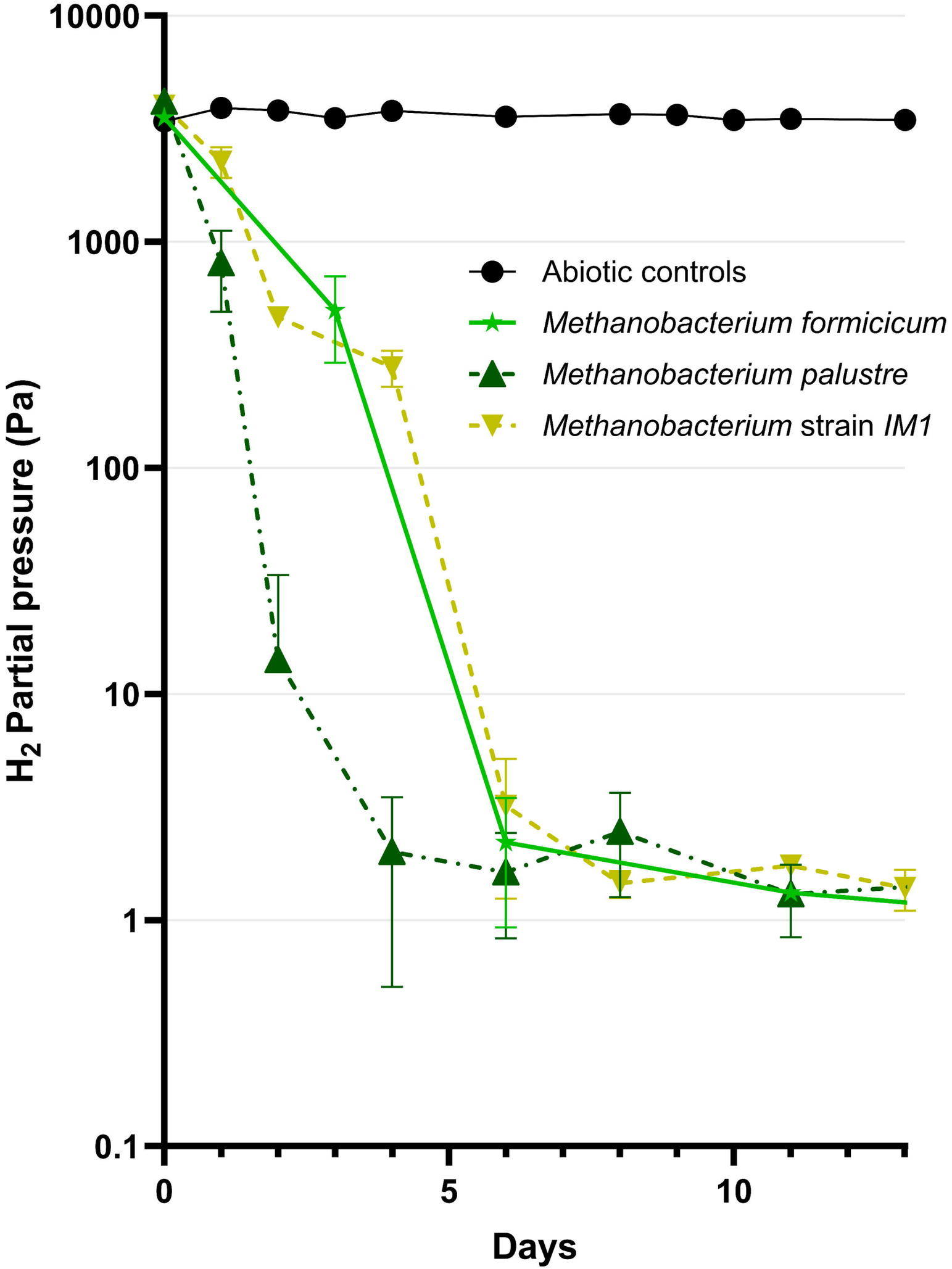
10000
1000
100
10
1
0.1
H_2 Partial pressure (Pa)
0
5
10
Days
Abiotic controls
Methanobacterium formicicum
Methanobacterium palustre
Methanobacterium strain *IM1*

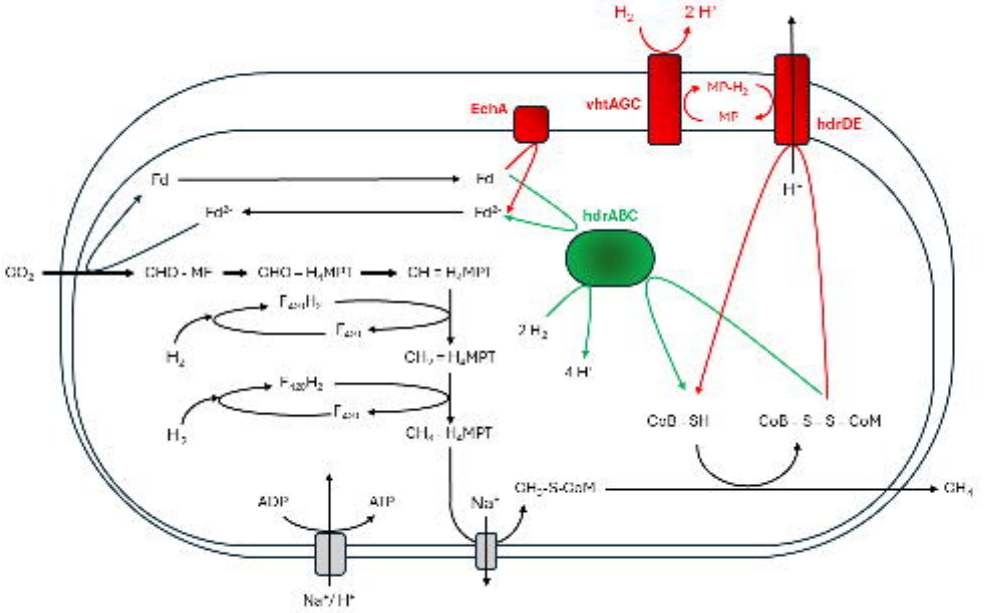
H2
2 H+
vhtAGC
MP-H2
MP
hdrDE
EchA
Fd
Fd
Fd2-
Fd2-
hdrABC
H+
CO2
CHO - MF
CHO - H4MPT
CH = H4MPT
2 H2
4 H+
H2
CH2 = H4MPT
H2
CH3 - H4MPT
CoB - SH
CoB - S - S - CoM
CH3-S-CoM
CH4
ADP
ATP
Na+
Na+/H+

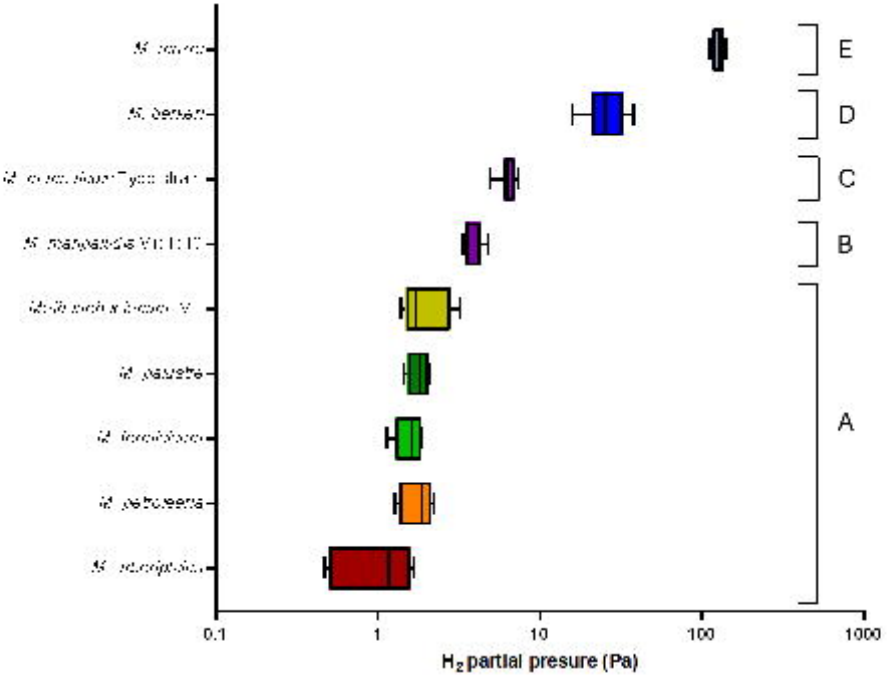
E
D
C
B
A
0.1
1
10
100
1000
H2 partial presure (Pa)

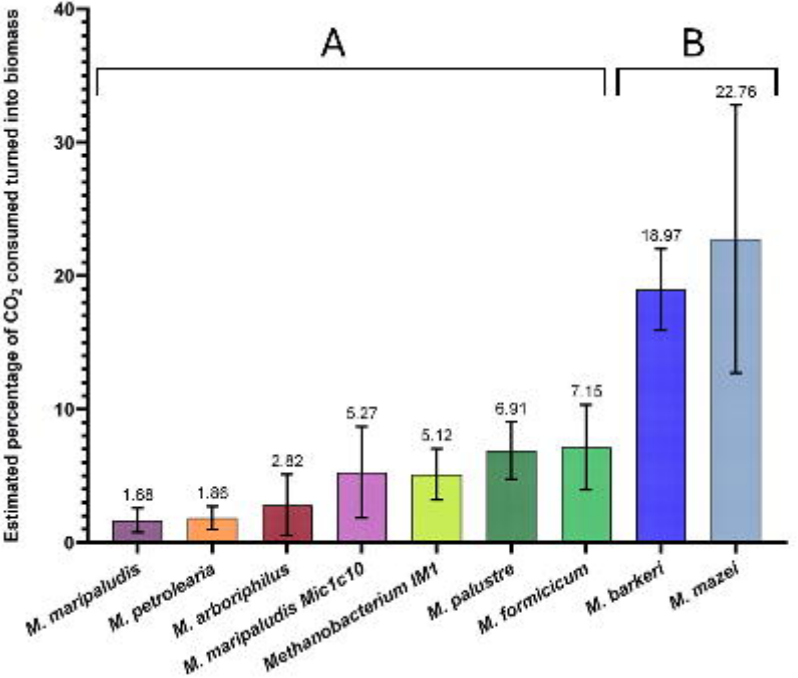
A
B
Estimated percentage of CO_2 consumed turned into biomass
40
30
20
10
0
1.68
1.88
2.82
5.27
5.12
6.91
7.15
18.97
22.76
M. maripaludis
M. petrolearia
M. arboriphilus
M. maripaludis Mic1c10
Methanobacterium IM1
M. palustre
M. formicicum
M. barkeri
M. mazei